Converting Core Sand Binder Processes in the Virtual World, Real Benefits in the Real World

Nigel P Yeomans, Jesus Benavente Jr,
Ashland Performance Materials, Dublin, Ohio, U.S.A.

ABSTRACT

For the past thirty years, many cores have undergone a conversion from the shell (Croning) production process to the phenolic urethane cold box process. It is widely accepted that the PUCB process is generally more productive than the heat-cured shell process and the vast number of cores converted over the years is a testament to that. The remaining cores that are still produced using the shell process are sometimes difficult cores to produce, often have some unique property that lends itself to the shell process or have been a victim of under investment. This paper outlines the process undertaken by one foundry to optimize the process of converting a shell core to a cold box core using computational fluid dynamics software to design the new process. The motivation behind this approach was to optimize the new production method at the same time as minimizing process method changes and financial investment. This approach also builds confidence in the process before the investment is made and leads to the greatest probability of success.

INTRODUCTION

A complex core for a hydraulic valve body is currently produced using the shell process. New tooling and a design change to the printing method provided the opportunity to improve productivity and reduce the cost of the core by converting the core making process to a phenolic urethane cold box process cured with amine. In many cases, it is possible to produce shell cores using cold box materials without changing the method of introducing sand into the tooling, changes to the venting arrangement are often essential to permit the catalyst gas to disperse throughout the core efficiently. Due to the complexity of this core (Figure 1) the process of redesigning the method was carried out using process simulation software designed for the core blowing process. The core geometry lends itself to be produced in a vertical core box and the proposed cold box core will be produced on a CB22 core machine.

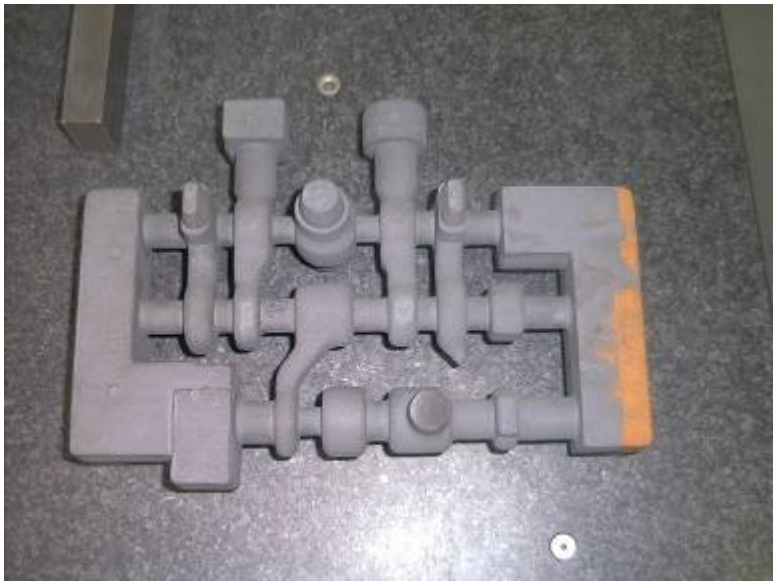

Figure 1. Hydraulic valve body core is shown in the above figure.

DEFINING THE PROCESS MODEL

The computer model begins with CAD geometry of the core which is used to create the computational mesh. The existing shell sand method for the core utilized a large invests area for the sand as shown in Figure 2. The difference in flowability between binder coated sand and shell sand would cause the sand to compact prematurely in the top core print area so it was decided to use three smaller invest areas (Figure 3).

Figure 2. This illustrates the Shell core invest method.

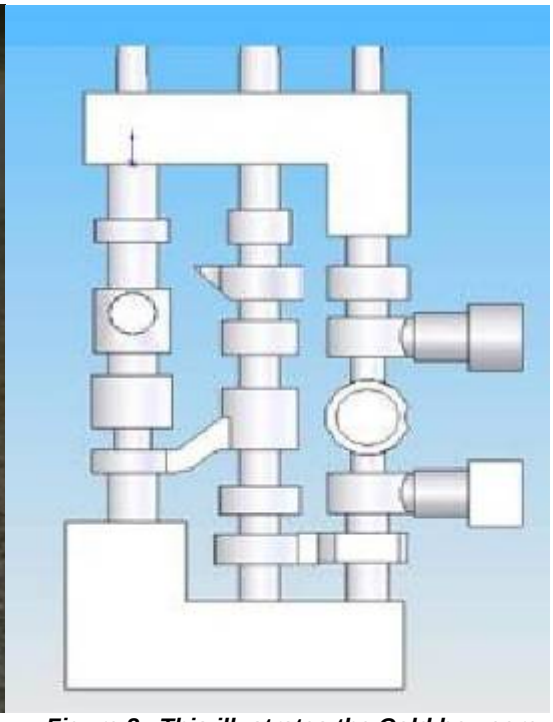

Figure 3. This illustrates the Cold box core invest method.

The core blowing process is an interaction of air and sand. Aerodynamic drag causes the sand to move from the sand magazine to the tooling and the sand displaces air as it fills the tooling. The software used to create the computational model is a multi-phase computational code which calculates the air flow using a Eulerian mesh and the sand grains using a Lagrangian mesh with a fully coupled solver.[1,2] This multi-phase method accurately predicts the particle behavior as described in previous papers on sand core process simulation. [3, 4, 5, 6, 7]

The process modeling was completed as three distinct calculations. The first calculation was used to identify the air movement within the tooling, the second calculation modeled the particle and air flow during the core blowing process and the third calculation modeled the transient gassing process as the amine catalyst is dispersed throughout the core.

AIR FLOW CALCULATION

This calculation is modeling the air flow through the tooling which is assumed to be full of sand. The run time on this calculation was 14 minutes; which enabled several iterations to be studied in order to optimize the vent locations in a short space of time. The key to any core blowing and gassing process is directional air flow of significant volume and velocity to impart sufficient aerodynamic drag on the sand particles. Insufficient drag will not compact the sand into the tooling causing poorly compacted regions which will affect casting surface finish and integrity.

The boundary conditions for the air flow calculation consist of a constant pressure applied to the top of the blow tubes and the process vents specified as discrete boundary conditions. The vent boundary conditions will carry over to the transient blowing calculation and the transient gassing calculation.

Figure 4 shows the computed results of the air flow calculations. The vent layout is modified based on the results of each calculation until the air flow and velocity is optimized. The iterative process of moving, adding or removing vents in this way took approximately one hour to complete; the improvement in air flow can be seen in Figure 4. The core to the left was the initial calculation and the core on the right is the optimized vent layout which shows significantly more air flow. The areas highlighted in blue show regions of the core box cavity with air velocity less than 0.2m/s.

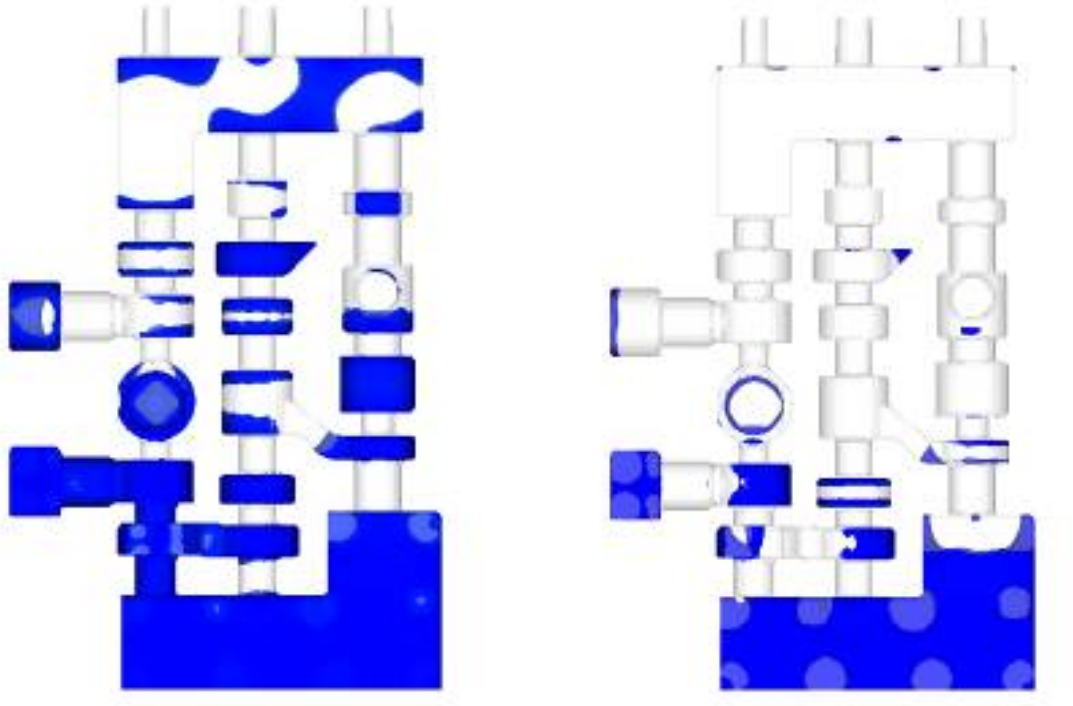

Figure 4. Air flow calculation results are shown in the above figure.

The optimum vent layout determined by the air flow analysis is shown in Figure 5 and Figure 6. All of the vents act as exhaust vents during the blowing process and allow the process air (air used to move the sand into the core box) and displaced air (atmospheric air already present in the core box) to exit the core box. The vents colored green are gassing inlet vents and allow catalyst gas to enter the core box during the curing process.

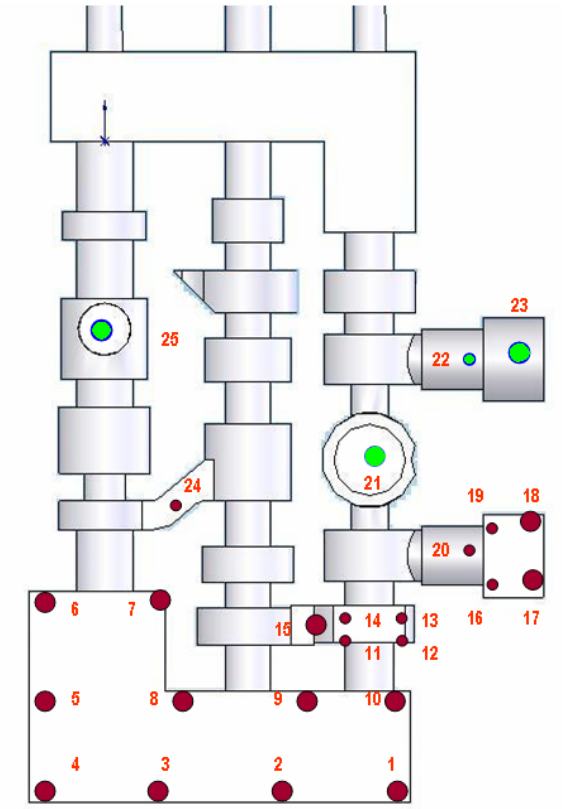

Figure 5. This illustrates the fixed platen vents.

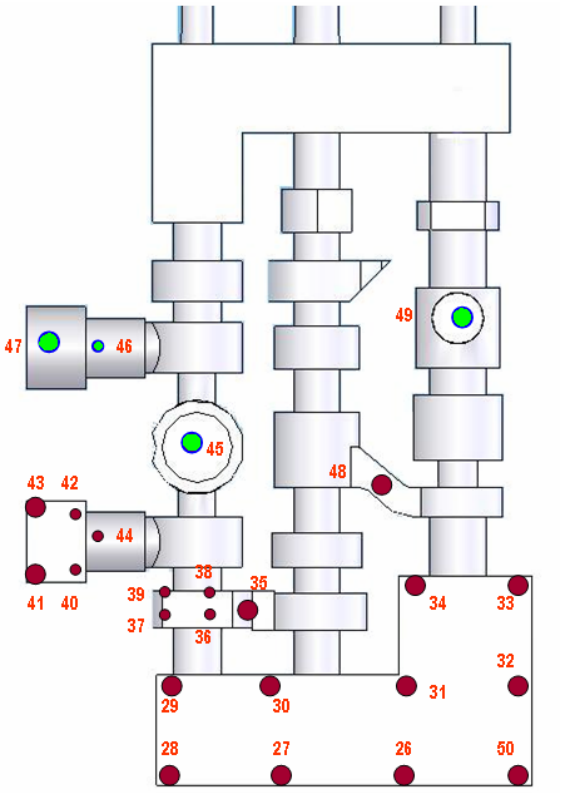

Figure 6. This illustrates the moving platen vents.

TRANSIENT CORE BLOWING CALCULATION

The transient core blowing calculation takes significantly longer to run than the air flow calculation. Having used the air flow calculation to optimize the initial method design, the required iterations of transient calculations can be reduced allowing for a faster turnaround of a new method. For this calculation a small section of the blow plate region of the process has been included in the mesh (Figure 7). Sand will be initialized in the blow plate region and the blow tubes at the start of the calculation. As sand moves from the blow plate region into the core cavity the calculation will allow more sand to enter the top of the calculation. By including the blow plate region in the calculation the sand enters the calculation in a region that is subject to low air and particle velocities. The blow tubes exhibit high air and sand velocity, therefore allowing sand to feed into the calculation domain at this point may cause instabilities in the flow solver.

The pressure boundary condition for this calculation is slightly more complex. A transient pressure is applied to the cells at the top of the blow plate region by taking data from a pressure file to describe the pressure increase from 0 Pa to full blow pressure versus time (Figure 8). The pressure is then held at the blow pressure for the duration of the calculation. The maximum designed blow pressure for this method was 300,000 Pa (3 bar). The vent boundary conditions were imported directly from the final air flow calculation.

Sand is specified by particle distribution and density. The sand particles are loaded into the blow plate and blow tubes by taking random particles from the sieve analysis for the process sand. As more sand enters the calculation, it is also taken randomly from the sieve analysis (Figure 9 and Figure 10).

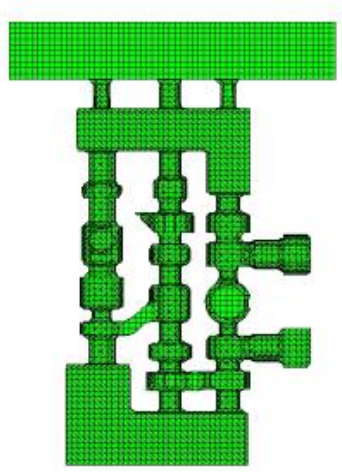

Figure 7. This illustrates computational mesh.

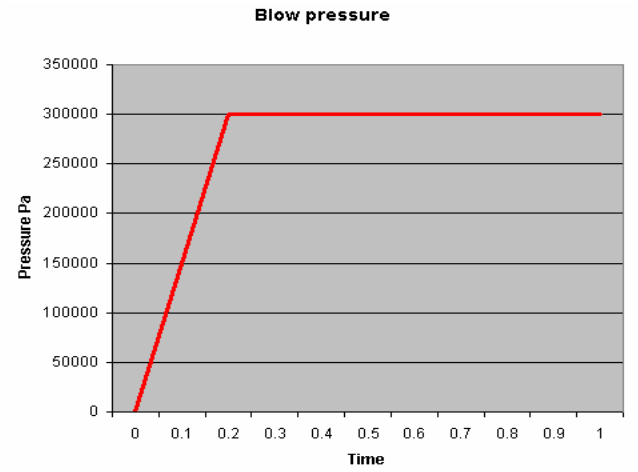

Figure 8. This graph illustrates blow pressure versus time.

Percent by wt	Radius (m)	Density (kg/m3)
0	6.34E-04	2760
1	3.59E-04	2760
11	2.54E-04	2760
34	1.79E-04	2760
36	1.27E-04	2760
16	8.97E-05	2760
2	6.35E-05	2760
1	4.47E-05	2760
0	3.18E-05	2760

Figure 9. This illustrates sand distribution.

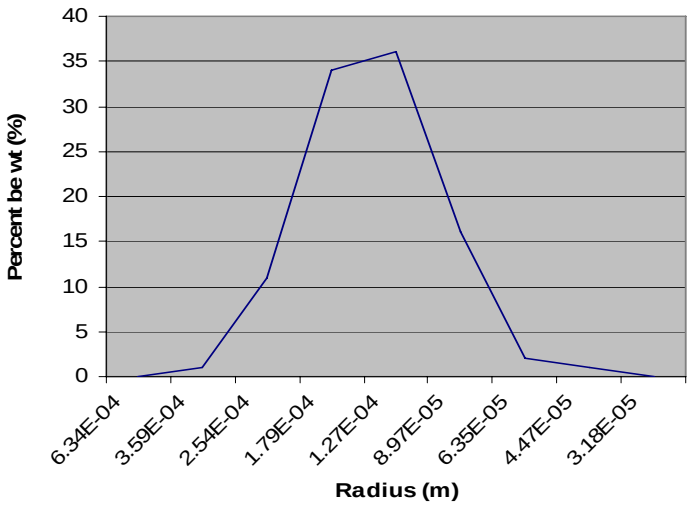

Figure 10. This graph illustrates sand distribution.

The results of the transient blowing calculation are shown in Figures 11 - 13. Changing the process to three small invest areas, instead of the one large invest which was used on the shell core, allows the sand to pass through the cylindrical sections of the core without compacting at the section changes. The sand begins to compact in the lower print area first and back fills towards the blow tubes, compacting into the remote areas in a sequential manner.

Figure 11. This illustrates core filling sequence.

At time 0, the core is empty of sand. At 0.1 seconds the sand can be seen flowing through the cylindrical sections of the core without compacting significantly at the section changes. At 0.2 seconds, the sand is compacting in the lower print area and back filling towards the blow tubes.

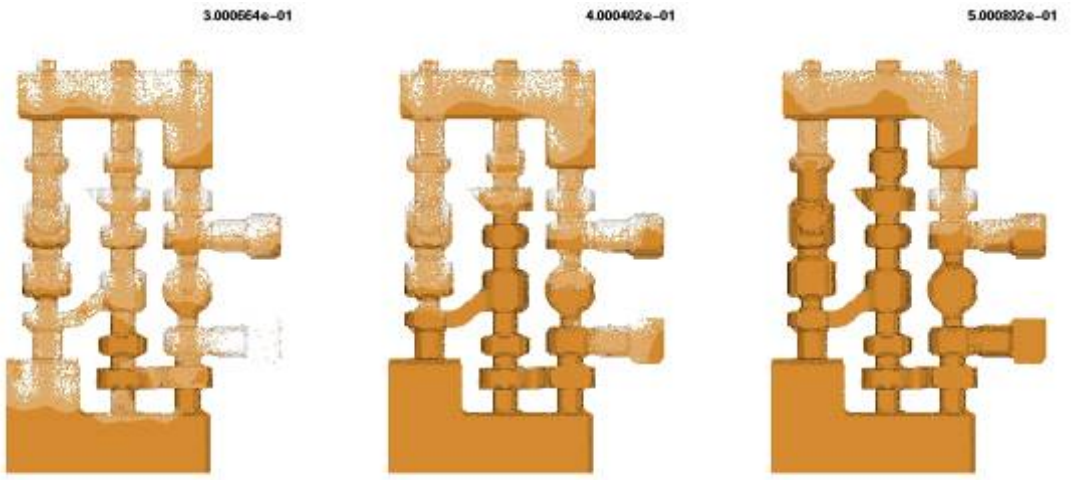

Figure 12. This illustrates core filling sequence.

After 0.3 seconds the lower print is compacting and sand is beginning to compact into the cylindrical sections. At 0.4 seconds the central cylindrical section is well compacted in the lower half. The outer cylindrical sections have not filled to the same degree due to the volume of sand in the lower print on the left hand side and the features on the right hand cylindrical section.

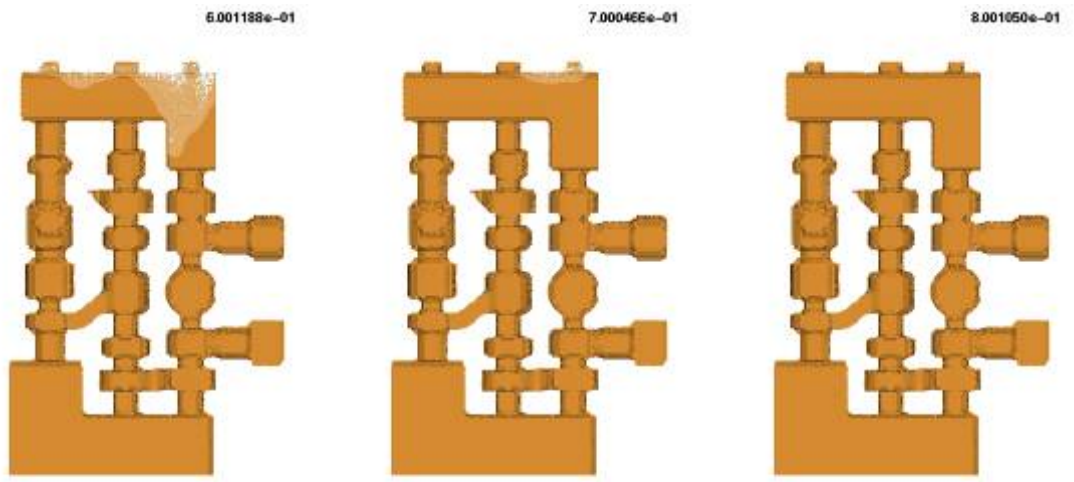

Figure 13. This illustrates core filling sequence.

By 0.6 seconds the cylindrical sections and features are completely filled. The upper print is filling with a bias to the left hand side due to the additional volume of sand on the right. At 0.8 seconds the core is completely filled.

The process is constantly changing during the filling cycle due to the effects of sand on the air flow. The efficiency of each vent changes as sand fills the core box cavity and the air flow changes velocity and direction based on the sand flow. Figures 14 and 15 demonstrate the constantly changing conditions with the core box during the blowing cycle.

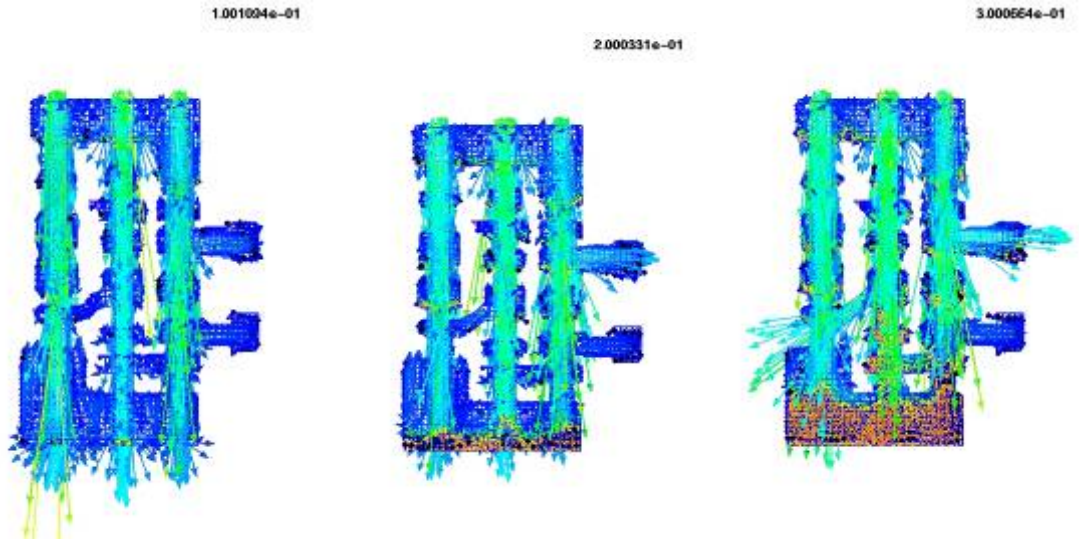

Figure 14 . This illustrates sequential air velocities.

At 0.1 seconds, the air is moving down the three cylindrical sections. The air velocity is averaging 20 m/s at this time. At 0.2 seconds, some of the vents in the bottom of the core are covered with sand which causes the air velocity to reduce to 15 m/s average and some of the air flow is diverted out of the vents in the features on the right hand side as viewed. At 0.3 seconds, the air flow begins to exit the core box through the vents in the midsection of the core as the efficiency of the lower vents reduces due to the packed sand in the lower print.

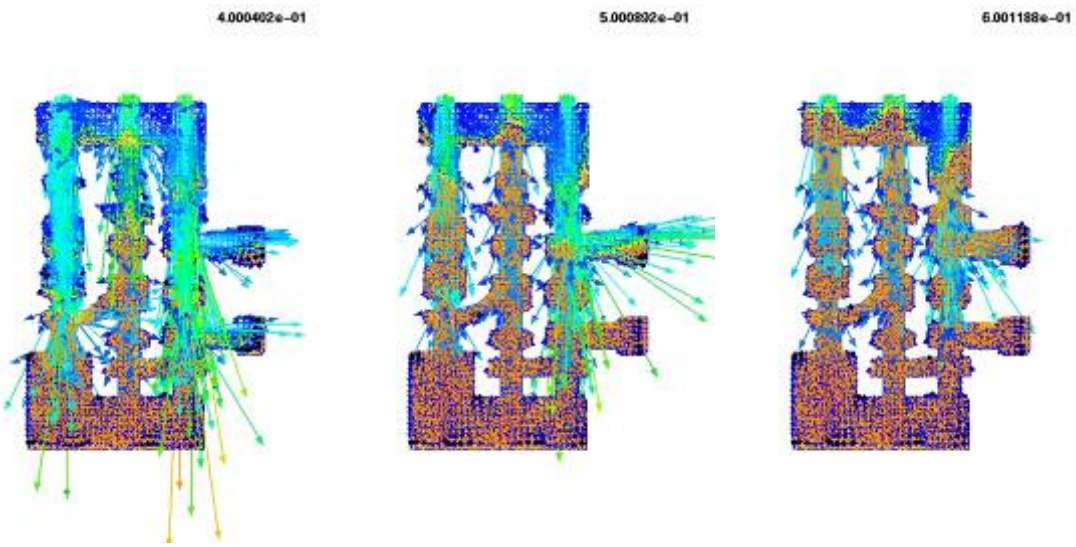

Figure 15. This illustrates sequential air velocities.

By 0.5 seconds most of the air is exiting through the vents on the extreme right as viewed. At 0.6 seconds, the two features on the right are full of sand which causes the air flow to exit through the midsection vents until the core is full. As the final third of the core fills, the air velocity reduces to 5 m/s average.

The conclusion from the transient blowing calculation is that the core will fill uniformly with the last part to fill being in the upper print area at 0.8 seconds. The predicted volume fraction of the sand shows a uniform density throughout the core ranging from 0.57 to 0.6 (figure 16). The maximum close pack fraction possible for the sand grade is 0.63 which is established by measuring the minimum volume of a known weight of the sand.

Tooling wear predictions (Figure 17) predict the areas of highest tool wear in the section change areas, some wear may also be evident in the right hand side of the upper print. The energy applied to specific areas of the tooling surface is calculated from the density of the sand, the velocity of the sand and the number of sand grains that impact the tooling surface during the blowing cycle. The calculated impact is also weighted by the angle of impact. Sand impacting the tooling surface at 90 degrees does less damage to the tooling surface than sand impacting at 37 degrees. Figure 16 shows the impact weighting applied for various angles.

Insufficient data exists to be able to predict a quantifiable amount of tool wear relative to the pattern material; however, the tool wear prediction is a valuable tool when comparing method designs.

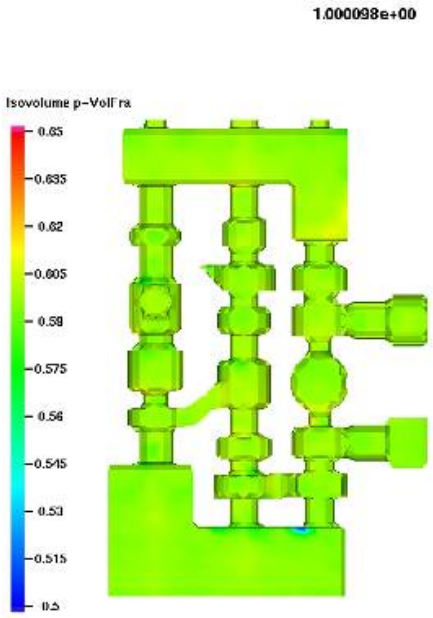

Figure 16. Computed final core is illustrated.

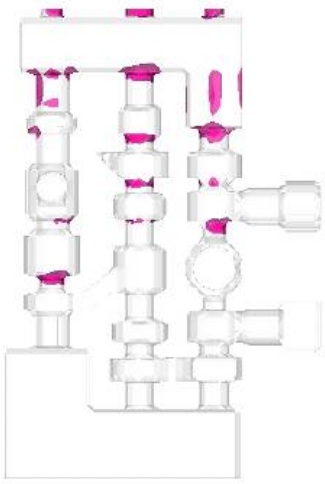

Figure 17. Computed tool wear is illustrated.

TRANSIENT CURING CALCULATION

The final part of the process is the curing cycle. The software will accurately calculate the progression of the catalyst gas through the core during this process. The actual cure is not calculated as this will depend on the binder and catalyst chemistry; the software does not calculate the chemical reaction process.

The vent boundary conditions are imported from the previous calculations and the pressure boundary condition is applied to the top of the invest area to replicate the gassing and purging process conditions. The pressure boundary conditions are also applied to the vents that are designated as “gassing” vents (Figures 6 and 7). This will allow air and catalyst to enter the calculation domain at these vents.

Figure 18 shows the transient progression of catalyst gas through the core during the curing process. Initially, amine enters the core through the sand invest areas and through the “gassing” vents midway down the core. Amine is allowed to enter the core in the mid region in order to prevent gas exiting the process as this would waste amine and also prolong the gassing cycle. The late stages of the gassing cycle show the last areas to receive gas are the lower print region and the region between the sand invest and the “gassing” vents on the right hand side as viewed. Depending on the permeability of the sand, it is theoretically possible to distribute the amine throughout this core in 8 – 10 seconds.

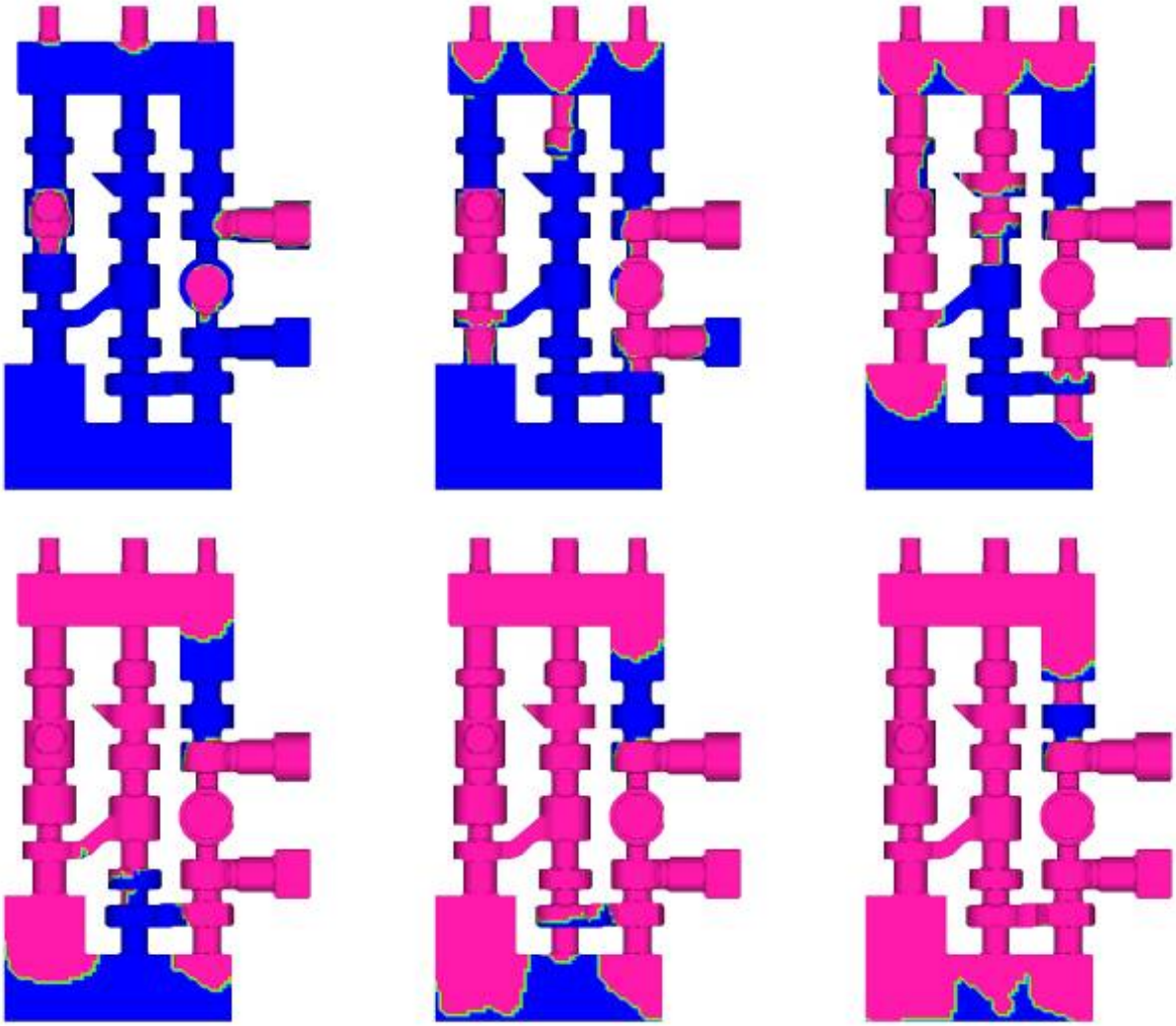

Figure 18. Computed transient gassing images are illustrated in this figure.

FOUNDRY TRIALS

The acid test for the new tooling and method design is blowing and curing cores in the foundry[8]. Despite some last minute design changes to increase the print sizes significantly, the core production went well. The cores were produced from the first blow cycle (Figure 19) and some additional vents were added to the enlarged print areas to improve compaction in the areas that had not been incorporated into the computational model. Initial casting trials with the new cores are under way at the time of writing this paper. The initial trial castings are shown in Figure 20.

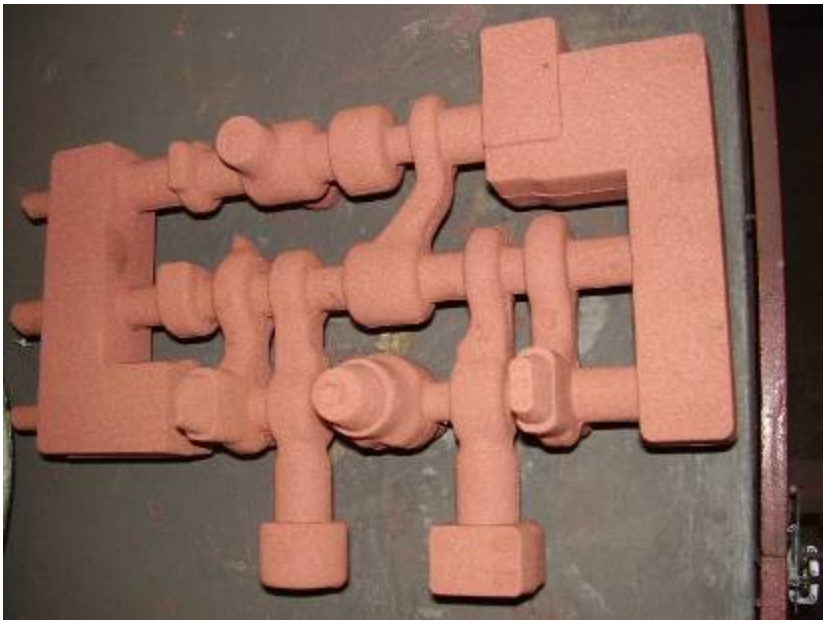

Figure 19. First core produced is shown in the above figure.

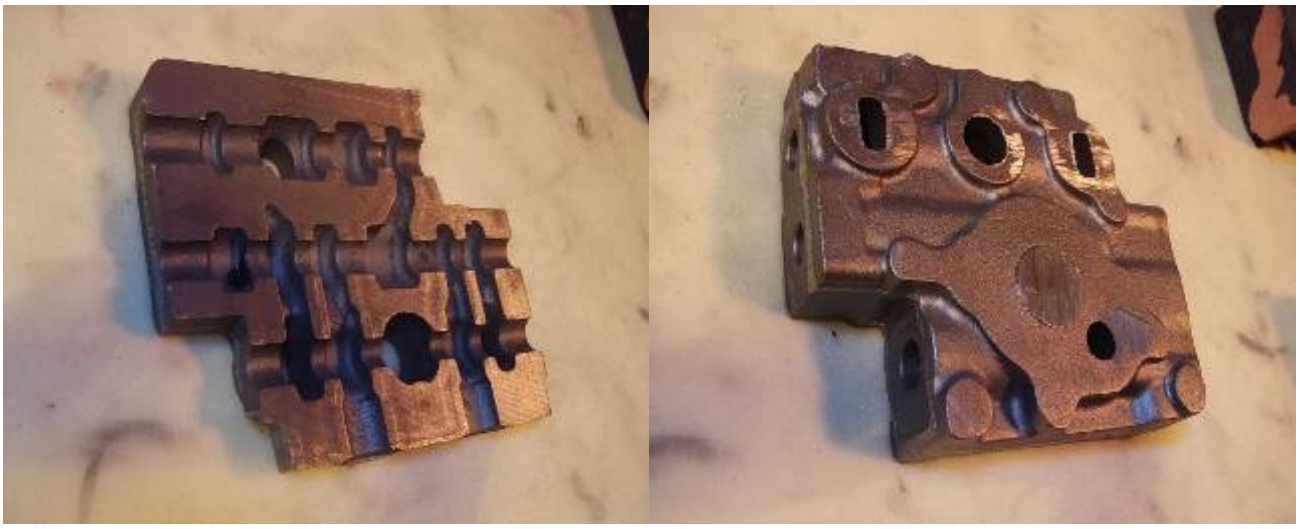

Figure 20. This figure illustrates initial casting.

PROCESS BENEFITS

A comparison of the cycle times between the cold box and the shell process is contained in Table 1. The shell core was produced on a U-180 core machine; the cold box core was produced on a CB-22 core machine.

Changing the production process for this core from shell sand to cold box resulted in cost savings for the foundry of $3.71 per core [9].

Table 1. Process Cycle Time Comparisons

Process	Blow time (s)	Gas time (s)	Purge time (s)	Cure time (s)	Total time (s)	Anticipated Cores per hour
Shell	2	n/a	n/a	35 – 70 (52 ave)	54	42
Cold Box	3	3	18	n/a	24	66

CONCLUSION

CFD software is commonplace in many modern foundries; the next logical step for process engineers is to extend computational modeling to more areas of their process. Doing so will enable a better understanding of the processes and will enable the foundry engineer to define more robust methods for each part of the foundry process. Modeling the core making process is a commercially viable process in terms of cost and time. The cost savings associated with projects, such as the one described in this paper, are significant and the knowledge base that is also added to the engineering staff from core production analyses is invaluable in the short- and long-term future.

REFERENCES

1. Andrews, M. J., and O'Rourke, P. J., 1996, "The Multiphase Particle-in-Cell (MP-PIC) Method for Dense Particle Flows," *International Journal of Multiphase Flow*, 22, pp. 379-402.
2. Snider, D. M., 2001, "An Incompressible Three-Dimensional Multiphase PIC Model for Dense Phase Flows," *Journal Of Computational Physics*, 170, pp. 523-549.
3. Blaser, P., Yeomans, N.P., "Sand Core Engineering and Process Modeling" Japanese Foundry Society, Nagoya, (November 2005).
4. Yeomans, N., Blaser, P., 2006, "Predicting the process," *Foundry Management and Technology*, pp 48-49 (January 2006).
5. Williams, K. A., Snider, D. M., Walker, M., Palczewski. 2002, "Process Modeling: Sand Core Blowing," *AFS Transactions* 02-141.
6. Walker, M., Palczewski, S., Snider, D., and Williams, K., 2002, "Modeling Sand Core Blowing: Simulation's next Challenge". *Modern Casting*, pp. 41-43 (April 2002)
7. Buchholz, A., Showman, R., Snider, D. "Experiences with Modeling the Core Blowing Process".
8. Cores and castings are in production at a North American Ductile Iron Foundry.
9. Financial data provided by the North American Ductile Iron Foundry producing the castings.